33rd Annual International Conference of the IEEE EMBS
Boston, Massachusetts USA, August 30 - September 3, 2011

Electrical-Thermal-Structural Coupling Simulation for Electrosurgery Simulators

Yoshihiro Kuroda, Shota Tanaka, Masataka Imura, Osamu Oshiro

Abstract— **An electrosurgery is a fundamental operation that utilizes Joule heat generated by the passage of a radiofrequency current. Surgical simulators are demanded for training of the electrosurgical skill with fewer complications. However, foregoing simulators have never implemented a series of physics phenomena in electrosurgery. The aim of this study is to construct a surgical simulator with a unified physics-based modeling of whole processes of electrosurgery. In this paper, we developed an electrosurgical cutting simulation system with consideration of a series of physical phases: electrical, thermal, and structural phases. Especially, the structural change based on the vaporization and mechanical rupture is modeled. The experiments using porcine livers compared the simulated temperature change with the measured one in electrosurgical cutting, and the effectiveness of the proposed model was found. In addition, the rate-controlling step for real-time electrosurgery simulation was examined.**

I. INTRODUCTION

THE demand of surgical simulation for clinical training has been stressed for the past decade, since the risk of surgical complications is linked to the surgeon's surgical technique, fundamental knowledge of the instrument, and so on[13]. Recently, objective assessment of surgical skills using commercial simulators[4] reported the usefulness of the simulators[10]. The electrosurgery is a fundamental operation and over 90 percent of all surgeries utilize electrosurgery in Minimally Invasive Surgery(MIS)[12]. The electrosurgery consists of a series of physical phases: electrical, thermal, and structural phases, as shown in Fig.1. However, the implemented electrosurgery simulation in surgical simulators ignored underlying physical phenomena and determined the area of material removal from the geometrical contact with the electrode or the temperature reaching 100 °C[6], [7], [8], because of the complexity of the phenomena and the required high update rate (graphics:>30Hz, haptics:>300Hz). On the other hand, biophysical mechanisms in electrosurgery remain under investigation[5]. The destruction of biological tissue is thought to be based on the vaporization caused by resistive heating. Several studies pointed out that the material destruction is caused from the mechanical rupture[11]. The surgical simulator with consideration of underlying physical phenomena enables residents to obtain the applicable knowledge of the instrument and to train an electrosurgical skill with fewer complications.

The aim of this study is to construct a surgical simulator with a unified physics-based modeling of whole processes of electrosurgery. In this paper, we propose an electrosurgical cutting simulation system with consideration of a series of physical phases. Especially, the structural change based on the vaporization and mechanical rupture is modeled. The experiments using porcine livers compare the simulated temperature change with the measured one in electrosurgical cutting. To our knowledge, the rate-controlling step in electrosurgery simulation has not yet been investigated. In this paper, calculation time of each process is measured to find the rate-controlling step for real-time electrosurgery simulation.

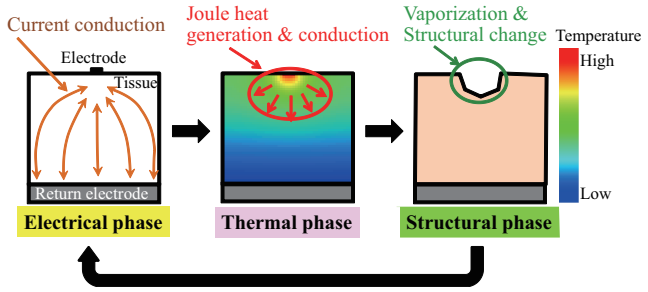

Fig. 1. A series of physical phases in electrosurgery

II. PHYSICS-BASED MODELING OF ELECTROSURGERY

A. Electrosurgical unit

An electrosurgical unit is a device for cutting soft tissue by Joule heat caused by a highly frequent current. The electrosurgical unit is illustrated in Fig.2. The probe is collided with tissue with a small contact area with the RF current. The Joule heat is high at the smaller contact area between the probe and the body, while the Joule heat is low at the return electrode, where the contact area is large. The pure cut and coagulation is conducted by changing the duty cycle of the waveform with the electrodes. In this paper, the pure cut is simulated, mainly to examine the calculation time.

B. Electrical and thermal phases

The electrical phase determines the current density distribution caused by the contact between the the electrosurgical probe and the object assuming the object being contact with a return electrode. The thermal phase determines the temperature distribution caused by Joule heating and temperature conduction. The governing equations of electric conduction and heat transfer are given by Laplace and heat

Graduate School of Engineering Science, Osaka University
Y. Kuroda, S. Tanaka, M. Imura, and O. Oshiro are with Graduate School of Engineering Science, Osaka University, Toyonaka 5608531, Japan
ykuroda@bpe.es.osaka-u.ac.jp

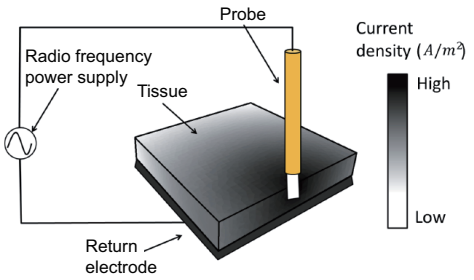

Fig. 2. Electrosurgical unit

equations.

$$\nabla^2 V = 0 \tag{1}$$

$$c\rho\frac{\partial T}{\partial t} = \lambda\nabla^2 T + \mathbf{J}\cdot\mathbf{E} \tag{2}$$

where V is voltage, T is absolute temperature, $\mathbf{J}$ is current density, $\mathbf{E}$ is electric field, and c, ρ, λ are specific heat, density, and thermal conductivity, respectively. Eq.1 gives electric potential distribution. Eq.2 calculates the temperature distribution.

C. Structural phase

The structural phase determines the structural change caused by vaporization and stress concentration. The stress is derived from the expansion of the volume caused by water vaporization. The volume expansion at the position $\mathbf{r}$ at the time t is given by

$$\triangle v(\mathbf{r},t) = \triangle v_{liq}(\mathbf{r},t) + \triangle v_{gas}(\mathbf{r},t) \tag{3}$$

where $\triangle v_{liq}(\mathbf{r},t), \triangle v_{gas}(\mathbf{r},t)$ are the expansion of water from the initial temperature and the expansion caused by the transition from liquid to vapor of water, respectively. The expansion leads the deformation and stress concentration. The equilibrium, strain-displacement relation, stress-strain relation, and constitutive equations are solved to calculate stress distribution. Finite Element Method(FEM) is used for the numerical solution. In the processes, Young modulus, Poisson's ratio, and breaking stress are considered. If the Mises stress is over the breaking stress, the elements in the area are removed to represent material destruction. The contact area between the probe and the tissue is updated from the moving direction of the probe, and the simulation was carried out repetitively by reconstructing the mechanical structure. The whole procedure is shown in Fig. 3.

III. Experiments

A. Experimental setups

The experimental measurement system was equipped with the electrosurgical unit (Conmed BIRTCHER 4400, monopolar), the electrical circuit to measure the voltage, and infrared thermography (Nippon Avionics CO., LTD., TVS-200, 60fps, 320 × 240 pixels, -20 to 300 °C range, 0.1 °C resolution) to measure the temperature change. Fig. 4 shows the measurement system. Porcine livers were cut for test samples. The size of the samples was 100 mm × 100 mm × 10 mm. The

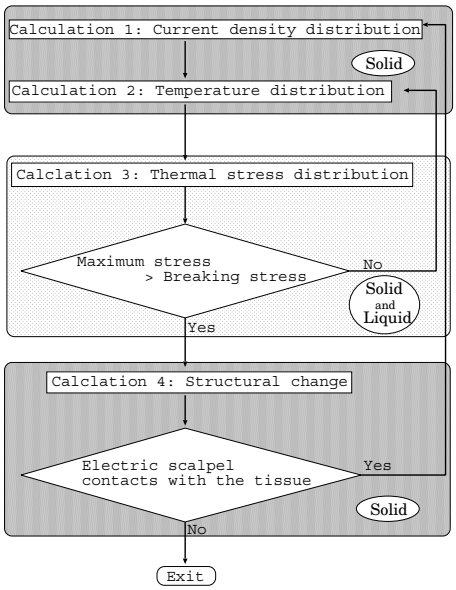

Fig. 3. The procedure of electrosurgical cutting.

simulation system was equipped with Intel CPU (Core2 Duo 2.66GHz), 3GB main memory, and nVidia GeForce GTX 295 graphics board. The object used in the simulation had 643 nodes (tetrahedral mesh). The object size was 100 mm × 100 mm × 10 mm. Table I shows the applied physical parameters, which are derived from the previous studies[1], [2], [3]. The size of the probe used in the simulation was 4 mm × 2 mm × 0.5 mm. The shape of the return electrode was a circle with a radius of 40 mm. In the simulation, the water evaporates at 100 °C, assuming that the effect of the stress on the vaporization is small enough to be ignored, although Ward points out that the increased stress makes the temperature of vaporization higher[11]. The boundary conditions in the simulation is given by Table II, where $\mathbf{n}$ is the normal vector, σ is the electric conductivity of the nodes, and λ is the heat conductivity.

TABLE I
Main physical parameters in the simulation

Specific heat × density	3.82 $\times 10^6 \mathbf{J}/(^\circ C \cdot m^3)$
Heat conductivity	0.502 W/(m·° C)
Electric conductivity	0.144 S/m
Young modulus	4.75 $\times 10^4$ Pa
Poisson's ratio	0.400
Critical stress	2.45 $\times 10^4$ Pa

B. Results and discussions

Experiments on electrosurgical cutting of porcine livers with an electrosurgical unit were performed. The measured images by thermography are shown in Fig.5. Fig.6 shows the simulation results of calculation phases: (a) distribution of the electric potential, (b) distribution of the temperature, and (c)distribution of the stress. Fig.7 shows the simulation

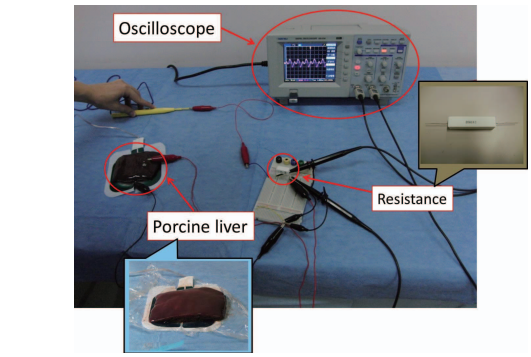

(a)

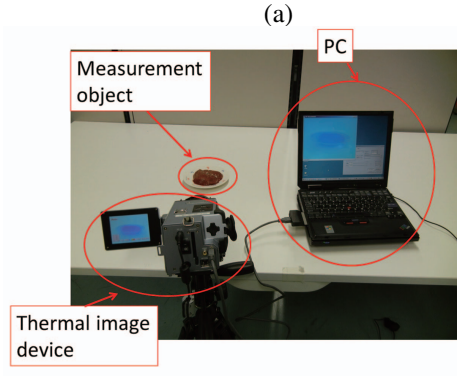

(b)

Fig. 4. Measurement system: (a)electrical circuit and (b)infrared thermography

TABLE II
BOUNDARY CONDITIONS IN THE SIMULATION

(a)Electrical phase

	Electric potential
Nodes contact with probe	V = 72 V
Nodes contact with return electrode	V = 0 V
Other boundary nodes	$\mathbf{n} \cdot (\sigma \nabla V) = 0$

(b)Thermal phase

	Temperature
Nodes contact with probe	$\mathbf{n} \cdot (\lambda \nabla T) = 0$
Nodes contact with return electrode	$\mathbf{n} \cdot (\lambda \nabla T) = 0$
Other boundary nodes	$\mathbf{n} \cdot (\lambda \nabla T) = 0$

results of continuous electro-surgical cutting by using the proposed method. The experimental data of measured temperature were compared with the simulation data as shown in Fig.8. The experimental data showed that the temperature went up over 100 °C up to around 140 °C and went down rapidly. However, the simulation data by using the foregoing method, which determined cutting region at 100 °C, showed that the temperature went up to around 100 °C and went down rapidly. This temperature change was different from the experimental data. The simulation data by using the proposed model, which determined cutting region with the stress derived from the vaporization, showed the repeated rise and fall over 100 °C. This temperature change was similar to the experimental data. The proposed model represented a feature of temperature change at the tissue destruction in

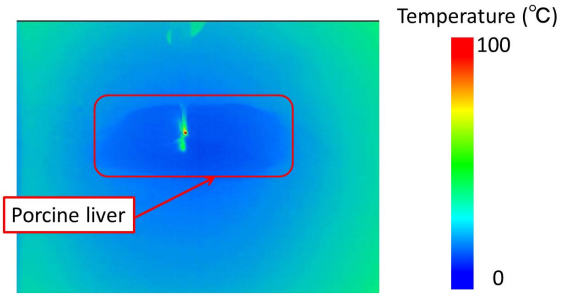

Fig. 5. Temperature distribution measured by thermography.

TABLE III
CALCULATION TIME

(a)Electrical and thermal phases [ms]

Number of nodes	257	506	1013	1507	2007
Matrix construction	9	19	43	67	96
LU factorization	1	12	87	302	672
Simultaneous equation solution	2	6	26	75	133
Total time	12	37	156	444	901

(b)Structural phase [ms]

Number of nodes	257	506	1013	1507	2007
Matrix construction	13	32	85	161	253
LU factorization	42	270	2062	6650	16161
Simultaneous equation solution	17	52	167	339	574
Total time	72	354	2314	7150	16988

electrosurgical cutting.

Table III shows calculation time for current density and temperature distribution, and stress distribution. Table III (a) shows calculation time for current density and temperature distribution, while Table III (b) shows the calculation time of stress distribution. The results showed that LU factorization accounted for a larger rate of total calculation time in both tables, as the number of nodes increased. When the number of nodes is 2,007, the ratio of LU factorization of the total calculation time becomes 75 % in the table (a), and 95 % in the table (b). The reason why the calculation time of LU factorization goes up rapidly compared with the solution of the simultaneous equation is that the computational complexity of the former is $O(N^3)$, while the complexity of the latter is $O(N^2)$, where N is the number of nodes. The results proved that the rate-controlling step in electrosurgery simulation was LU factorization. For real-time processing to achieve visual and haptic feedback, a solution for LU factorization should be reduced effectively. GPU computing is a promising approach to speed up the calculation of the process. It is reported that calculation time for physics simulation became one-thirtieth by GPU computing[14].

IV. CONCLUSION

In this paper, we developed an electrosurgical cutting simulation system with consideration of a series of physical phases: electrical, thermal, and structural phases. Especially, the structural change based on the vaporization and mechanical rupture was modeled. The experiments using porcine

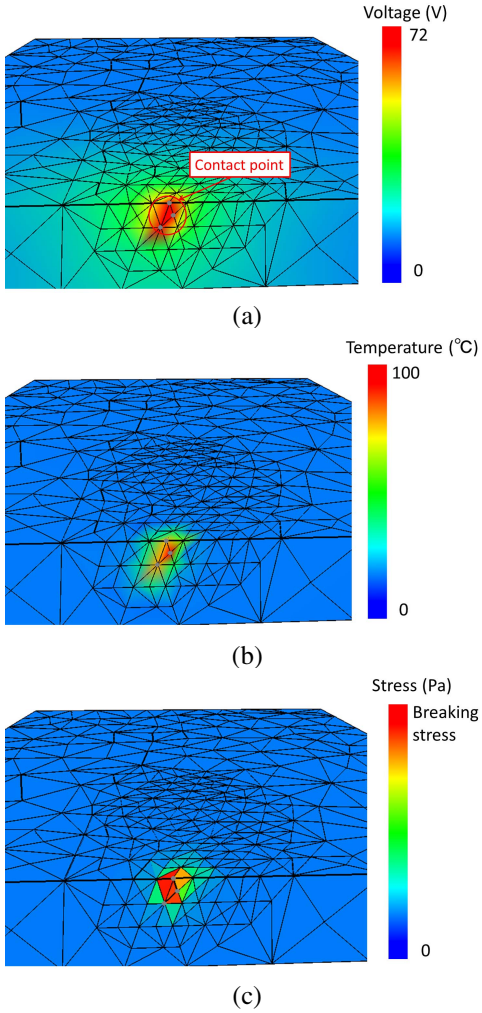

Fig. 6. Simulation results: (a) distribution of electric potential, (b) distribution of temperature, and (c)stress distribution

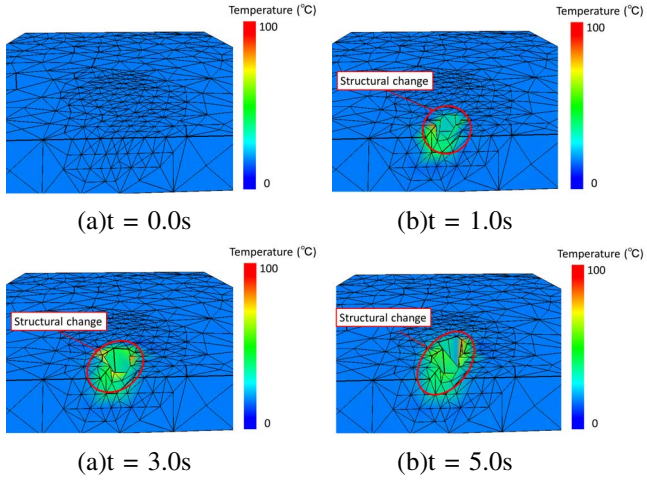

Fig. 7. Simulation results of continuous electro-surgical cutting

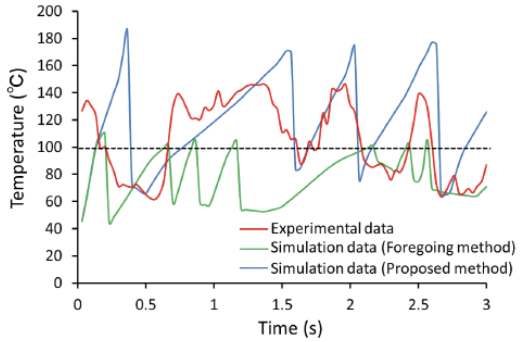

Fig. 8. Temperature change

livers compared the simulated temperature change with the measured one in electrosurgical cutting, and the effectiveness of the proposed model was found. In addition, the rate-controlling step for real-time electrosurgery simulation was found. Experiments on coagulation, which is important for preventing bleeding during surgical cutting, is a future work.

V. ACKNOWLEDGMENTS

This study was partly supported by the Global COE Program "*in silico* medicine" at Osaka University.

REFERENCES

[1] C. Gabriel, S. Gabriel and E. Corthout : The dielectric properties of biological tissues, *Physics in Medicine and Biology*, Vol.41, No.11, pp. 2231-2249, 1996.

[2] S.H. Oh, B.I. Lee, E.J. Woo, S.Y. Lee, T.S. Kim, O. Kwon and J.K. Seo : Electrical conductivity images of biological tissue phantoms in MREIT, *Physiological Measurement*, Vol.26, No.2, pp. 279-288, 2005.

[3] J.W. Valvano, J.R. Cochran and K.R. Diller : Thermal conductivity and diffusivity of biomaterials measured with self-heated thermistors, *International Journal of Thermophysics*, Vol.6, No.3, pp. 301-311, 1985.

[4] LapSim, Surgical Sicence Ltd., www.surgical-science.com, (referred 2011.3).

[5] E. Berjano: Theoretical modeling for radiofrequency ablation: state-of-the-art and challenges for the future, *BioMedical Engineering OnLine*, 2006.

[6] A. Maciel and S. De : Physics-based Real Time Laparoscopic Electrosurgery Simulation, *Medicine Meets Virtual Reality 16*, pp. 272-274, 2008.

[7] C.R. Chen, M.I. Miga, R.L. Galloway : Optimizing Electrode Placement Using Finite-Element Models in Radiofrequency Ablation Treatment Planning, *IEEE Trans. Biomed Eng.*, Vol 56, Issue 2, pp. 237-245, 2009.

[8] S. Cotin, H. Delingette and N. Ayache : A hybrid elastic model for real-time cutting, deformations and force feedback for surgery training and simulation, *The Visual Computer*, Vol 16, No.8, pp. 437-452, 2000.

[9] R.E. Dodde, S.F. Miller, J.D. Geiger and A.J. Shih : Thermal-Electric Finite Element Analysis and Experimental Validation of Bipolar Electrosurgical Cautery, *Journal of Manufacturing Science and Engineering*, Vol.130, Issue 2, 2008.

[10] C.R. Larsen, T. Grantcharov, R. Aggarwal, A. Tully, J.L. Sorensen, T. Dalsgaard, B. Ottesen: Objective assessment of gynecologic laparoscopic skills using the LapSimGyn virtual reality simulator, *Surg Endosc.*, Vol. 20, No. 9, pp. 1460-1466, 2006.

[11] A. Ward, C. Ladtkow, G. Collins: Material Removal Mechanisms in Monopolar Elecrosurgery, *IEEE EMBC*, pp. 1180-1183, 2007.

[12] Laparoscopic Electrosurgical Complications, www.encision.com (accessed 2011.04).

[13] C.H. Nezhat, F. Nezhat, I. Brill, C. Nezhat: Normal variations of abdominal and pelvic anatomy evaluated at laparoscopy. *Obstet Gynecol.*, Vol. 9, pp. 238-242, 1999.

[14] J. Mosegaard, T.S. Sorensen: GPU Accelerated Surgical Simulators for Complex Morphology. *Proceedings of IEEE VR*, pp. 147-154, 2005.